Spectroscopic study on the charge redistribution between Au and Ag in Au@Ag core-shell nanoparticles

S. Nishimura, D. T. N. Anh, D. Mott, K. Ebitani and S. Maenosono*

School of Materials Science, Japan Advanced Institute of Science and Technology,
1-1 Asahidai, Nomi, Ishikawa 923-1292, Japan, shinya@jaist.ac.jp

ABSTRACT

Charge transfer in Au nanoparticles (NPs) and Au@Ag core-shell NPs synthesized with a wet-chemical reduction method was investigated by X-ray absorption near-edge structure (XANES) and X-ray photoelectron spectroscopy (XPS) techniques. The electron depletion of Au 5*d* state in the Au@Ag$_x$ NPs compared to Au NPs was ascertained by the XANES analysis in Au $L_{2,3}$-edges though the Ag thickness (*x* nm), which affected the hole density of Au 5*d* states. The order of Au 5*d*-state hole density was confirmed as Au foil ≅ Au NPs < Au@Ag$_x$ NPs. The positive and negative shifts in the Au 4*f* and Ag 3*d* binding energies in XPS spectra of Au@Ag$_x$ NPs compared to Au or Ag NPs suggested that the Ag shell formation strongly contributes to the electron depletion of 5*d* state in Au atoms of the Au core. According to these results, we concluded that the electron transfer from Au to Ag in the Au@Ag heteromeric NPs followed the charge compensation mechanism.

Keywords: Au@Ag core-shell NPs, XANES, XPS, electron transfer, charge compensation mechanism.

1 INTRODUCTION

Heteromeric structured NPs are highly attractive for the development of advanced materials in various areas such as semiconductors, magnetic materials, sensors, and catalysts.[1-4] Heteromeric Au and Ag NPs are especially widely-studied for localized surface plasmon resonance (LSPR) and surface enhanced Raman scattering (SERS) based biomolecular sensing and diagnostics.[5-7] For example, Ag@Au core-shell NPs are considered a preferable sensing agent owing to their optical enhancement and chemical stability derived from Ag and Au, respectively. However, there remain challenges for construction of the Ag@Au NPs because the galvanic replacement reaction occurs between aqueous Au and metallic Ag during the Au shell deposition process.[8]

Very recently, we reported the synthesis of uniform Au@Ag core-shell NPs and (Au@Ag)@Au double-shell NPs, and their special performance such as the high oxidation resistivity of the Ag shell and strong Raman signal.[9,10] Interestingly, the formed (Au@Ag)@Au NPs exhibited a uniform Au second-shell, which indicated that the galvanic reduction was inhibited during the Au second-shell deposition onto the Au@Ag NPs. As the result of a negative shift in the Ag 3*d* area with positive shift in the Au 4*f* area of the X-ray photoelectron spectroscopy (XPS) spectra, we proposed that an electron transfer from the Au core to the Ag shell in Au@Ag NPs strongly contributed to the anti-galvanic reduction process.

Hearin, we employed X-ray absorption near-edge structure (XANES) analysis[11] in combination with XPS analysis using an asymmetric Gaussian-Lorentzian mixed function[12] to further investigate the charge transfer phenomenon in the Au@Ag heteromeric NPs.

2 EXPERIMENTAL

The Au and Au@Ag NPs were synthesized using a modified multi-step citrate reduction method.[9] Briefly, an aqueous solution of $HAuCl_4 \cdot 3H_2O$ (0.56 mM, 45 mL) was heated to reflux, then an aqueous solution of trisodium citrate trihydrate (SC) (1 wt%, 5 mL) was added into the boiling solution. After 1 h reflux, the Au NPs (14.4 nm) were obtained. The Au@Ag NPs was synthesized with the same procedure using Au NPs as a seed after the dialysis with membrane, respectively; *i.e.* the seed dispersed solution was refluxed with stirring, then SC and $AgNO_3$ were simultaneously added dropwise (Scheme 1).

Scheme 1 Synthetic route to Au and Au@Ag NPs.

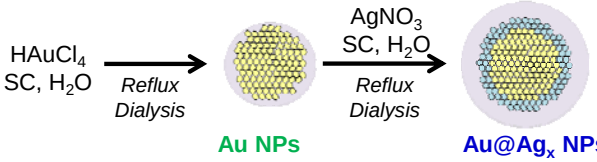

XPS (Shimadzu Kratos AXIS-ULTRA DLD), XANES (BL01B1, SPring-8, Japan, proposed No. 2011A1607), and other analytical techniques were performed for the characterizations. The white-line (WL) feature in L_2-edge XANES spectrum originates in the $2p_{1/2} \rightarrow d_{3/2}$ dipole-allowed transition where the L_3-edge is related to the $2p_{3/2} \rightarrow d_{3/2}$ and $2p_{3/2} \rightarrow d_{5/2}$ dipole-allowed transitions (Figure 1).[13] Therefore, the number of holes in the $d_{3/2}$ and $d_{5/2}$ orbitals above the Fermi level were able to be estimated from L_2- and L_3- edges XANES spectra.

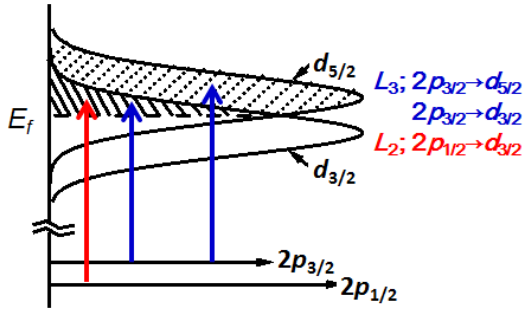

Figure 1 Schematic illustration of the electronic transitions.

The analysis of Au $L_{2,3}$-edge XANES spectra were followed Mansour's method.[14] Changes in the numbers of 5*d*-hole in Au atoms from those of Au bulk (Δh_d) were estimeted as the sum of $\Delta h_{3/2}$ and $\Delta h_{5/2}$;

$$\Delta h_{3/2} = h_{3/2,\mathrm{NPs}} - h_{3/2,\mathrm{bulk}} = \frac{3\Delta A_2}{C} \quad (1)$$

$$\Delta h_{5/2} = h_{5/2,\mathrm{NPs}} - h_{5/2,\mathrm{bulk}} = \frac{2.25\Delta A_3 - 0.5\Delta A_2}{C} \quad (2)$$

where A_i (eV·cm^{-1}) is the WL area for the L_i-edge XANES spectrum. The WL area was selected in the range from 10 eV below the X-ray absorption edge (E_0) to 13 eV above E_0. ΔA_i is the difference values between NPs and bulk. C = 75213 (eV·cm^{-1})[14,15] is the characteristic constant of the absorption.

3 RESULTS AND DISCUSSION

The synthesized Au and Au@Ag core-shell NPs showed narrow particle size distributions and no segregated atoms.[8]

3.1. Differences in XANES spectra between Au foil and Au NPs

The Au L_3-edge XANES spectra of Au foil (bulk) and Au NPs are shown in Figure 2. It was known that the kinds of capping agants increase or decrease the hole density of NPs due to their electronic effects (attractant or donation).[16,17] However, there seems to be no differences in the XANES spectra between Au foil and Au NPs. Oyama *et al.* reported that the 5*d*-hole density of Au atoms in Au NPs rarely changed for particle diameters above 10 nm even under the presence of electron attracting capping agent.[18] Furthermore, it has been reported that the critical size requirement of the Au NPs is below 5 nm, becoming prominent below 2 nm.[19,20] The mean diameter of the synthesized Au NPs was 14.4±0.7 nm, which is too large to exhibit electronic effects of capping agent and size-dependent effects. Therefore, the effects from capping agent and particle size were neglegible for investigation in the electron transfer of Au atoms in the Au and Au@Ag NPs.

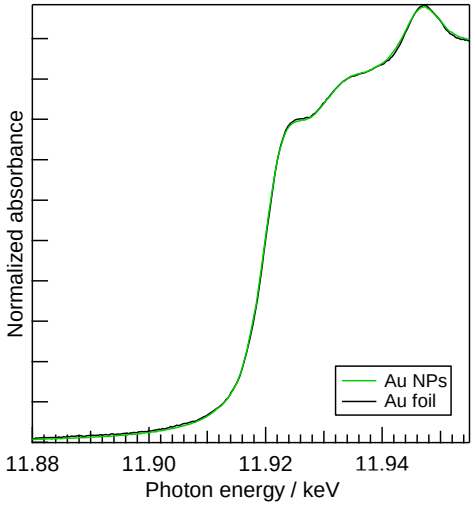

Figure 2 Au L_3-edge XANES spectra of Au foil and the synthesized Au NPs.

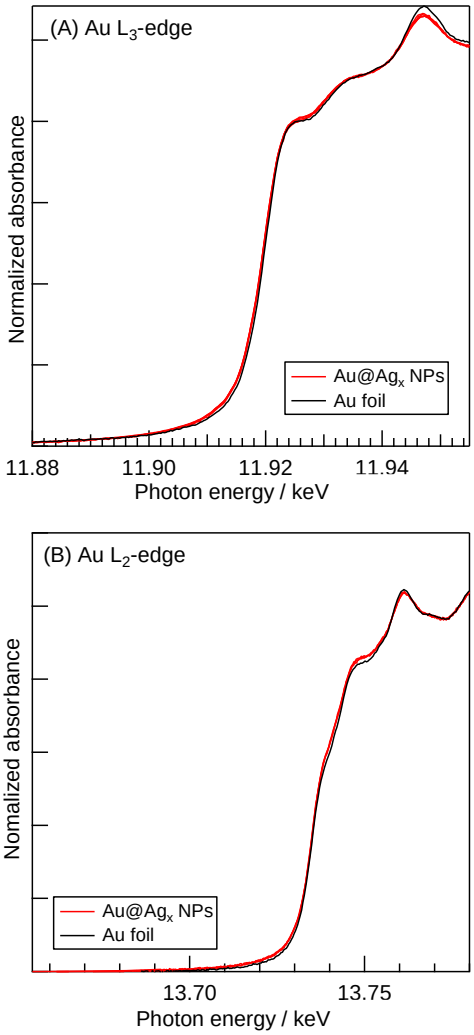

Figure 3 (A) Au L_3-edge and (B) Au L_2-edge XANES spectra of Au foil and the synthesized Au@Ag$_x$ NPs.

3.2. Effect of Ag thickness in Au@Ag NPs

The Au $L_{2,3}$-edge XANES spectra of Au@Ag$_x$ NPs with a Ag shell thickness (x) of 0.4±0.3, 1.0±0.6 and 2.2±0.4 nm are shown in Figure 3A and B. The XANES spectra exhibited identical shapes among Au@Ag$_x$ NPs in both Au L_2- and L_3- edges, indicating that the Ag thickness minimally affected the 5*d* hole density of the Au core. Moreover, the WL features of those spectra are higher than that of Au foil. These results supported that the Ag shell formation induced the electron depletion of Au 5*d* state. In fact, approximetly 0.03 holes in 5*d* state in a Au atom seemed to be increased; the parameters are sumarized in Table 1.

Table 1 Parameters obtained by XANES analysis

Sample[a]	ΔA_3 / eV·cm^{-1}	ΔA_2 / eV·cm^{-1}	Δh_d / atom^{-1}
Au@Ag$_{0.4}$ NPs	600.5	425.7	3.2×10^{-2}
Au@Ag$_{1.0}$ NPs	617.2	383.0	3.1×10^{-2}
Au@Ag$_{2.2}$ NPs	675.2	413.5	3.4×10^{-2}

[a] x denotes the mean Ag shell thickness (nm).

3.3. XPS analysis of Au@Ag$_x$ NPs

To further investigate the charge transfer effects, XPS spectra of Au@Ag$_x$ NPs were examined. The positions in the Au 4*f* and Ag 3*d* binding energies in XPS spectra, estimated with an asymmetric Gaussian-Lorentzian mixed function, are shown in Figure 4A and B with monometallic Au or Ag NPs. From comparisions between monometallic Au or Ag NPs and Au@Ag$_x$ NPs, the positions of Au@Ag$_x$ NPs in Au 4$f_{7/2}$ peaks shifted to the higher energy side than for Au^0 NPs (84.03 eV) whereas the Ag 3$d_{5/2}$ peaks shifted to the lower energy side when compared to Ag^0 NPs (368.26 eV). The positive and negative shifts in the Au 4*f* and Ag 3*d* binding energies in XPS spectra suggested that the electron transfer from Au to Ag in the heterometallic Au@Ag$_x$ NPs is consistently observed. Further comparision among Au@Ag$_x$ NPs indicated that the degree of the negative shifts in Ag 3$d_{5/2}$ peaks were gradually decreased; *i.e.* the negativity on Ag atoms gradually weakened with increasing the Ag thickness. It seemed that the electron transfer effect from Au to Ag atoms mainly is interfacial in nature.

3.4. Charge compensation mechanism

In the previous literature, Sham and co-workers have reported the charge compensation mechanism in a AuM_2 alloy series (M = Al, Ga, In, Sn, Sb, and Te).[15,21-25] According to the mechanism, the differences of Pauling's electronegativity between Au and host M element contributed to the degree of the electron transfer from Au to M; the Au gains electrons in the 5*d* and 6*sp* orbitals from the 5*d* orbital of M, thereafter, the electron disbalance between Au and M was compensated by the backdonation from the Au to M, then the charge onto M was overcompensated. According to our results, the charge compensation mechanism was also observed in the Au@Ag$_x$ NPs. The formed over-charged Ag (negatively charged) may inhibit the galvanic reduction during the Au second-shell deposition onto the Au@Ag NPs.

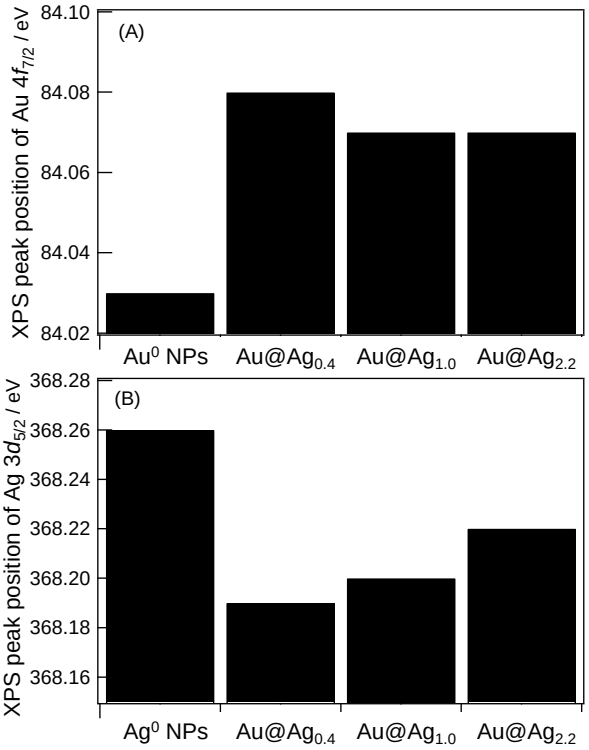

Figure 4 XPS binding energies of (A) Au 4$f_{7/2}$ and (B) Ag 3$d_{5/2}$ peaks for the synthesized Au@Ag$_x$ NPs with Au and Ag NPs.

4 CONCLUSION

The collection of XANES and XPS analysis evidenced the charge transfer from Au to Ag in the Au@Ag core-shell NPs based on the charge compensation mechanism, and the formed nagatively-charged Ag seemed to contribute to the anti-galvanic reduction process during the Au second-shell formation onto Au@Ag NPs. The quantum mechanical calculation is ongoing. These investigations may guide the advanced strategies for design of the properties in heteromeric NPs by using electronic structure control.

REFERENCES

[1] Y. Xia, Y. Xiong, B. Lim, S. E. Skrabalak, Angew. Chem., Int. Ed. 48, 60, 2009.
[2] A.-H. Lu, E. L. Salabas, F. Schuth, Angew. Chem., Int. ed. 46, 1222, 2007.

[3] M. E. Stewart, C. R. Anderton, L. B. Thompson, J. Maria, S. K. Gray, J. A. rogers, R. G. Nuzzo, Chem. Rev. 108, 494, 2008.
[4] H. Zhang, T. Watanabe, M. Okumura, M. Haruta, N. Toshima, Nature Mater. 11, 49, 2012.
[5] Y. Cui, B. Ren, J.-L. Yao, R.-A. Gu, Z.-Q. Tian, ., J. Phys. Chem. B 110, 4002, 2006.
[6] N. L. Rosi, C. A. Mirkin, Chem. Rev. 105, 1547, 2005.
[7] F. Frederix, J.-M. Friedt, K.-H. Choi, W. Laureyn, A. Campitelli, D. Mondelaers, G. Maes, G. Borghs, Anal. Chem. 75, 6894, 2003.
[8] D. Mott, J. D. Lee, N. T. B. Thuy, Y. Aoki, P. Singh, S. Maenosono, Jpn. J. Appl. Phys. 50, 065004, 2011.
[9] D. T. N. Anh, P. Singh, C. Shankar, D. Mott, S. Maenosono, Appl. Phys. Lett. 99, 073107, 2011.
[10] C. Shankar, T N D. Anh, P. Singh, K. Higashimine, D. Mott, S. Maenosono, under revison.
[11] S. Nishimura, A. T. N. Dao, D. Mott, K. Ebitani, S. Maenosno, J. Phys. Chem. C 116, 4511, 2012.
[12] S. Maenosono, J. D. Lee, A. T. N. Dao, D. Mott, submitted.
[13] N. F. Mott, Proc. Phys. Soc. A 62, 416, 1949.
[14] A. N. Mansour, J. W. Cook, D. E. Sayers, J. Phys. Chem. 88, 2330, 1984.
[15] C. C. Tyson, A. Bzowski, P. Kristof, M. Kuhn, R. Sammynaiken, T. K. Sham, Phys. Rev. B 45, 8924, 1992.
[16] P. Zhang, T. K. Sham, Appl. Phys. Lett. 81, 736, 2002.
[17] H. Hakkinen, R. N. Barnett, U. Landman, Phys. Rev. Lett. 82, 3264, 1999.
[18] J. Ohyama, K. Teramura, T. Shishido, Y. Hitomi, K. Kato, H. Tanida, T. Uruga, T. Tanaka, Chem. Phys. Lett. 507, 105, 2011.
[19] T. Ishida, M. Hatura, Angew. Chem., Int. Ed. 46, 7154, 2007.
[20] H. Tsunoyama, N. Ichikuni, H. Sakurai, T. Tsukuda, J. Am. Chem. Soc. 131, 7086, 2009.
[21] A. Bzowski, Y. M. Yiu, T. K. Sham, Phys. Rev. B, 51, 9515, 1995.
[22] T. K. Sham, M. L. Perlman, R. E. Watoson, Phys. Rev. B 19, 539, 1979.
[23] R. E. Watoson, J. Hudis, M. L. Perlman, Phys. Rev. B 4, 4139, 1971.
[24] W. Drube, R. Treusch, T. K. Sham, A. Bzowski, Phys. Rev. B 58, 6871, 1998.
[25] D. T. Jiang, T. K. Sham, P. R. Norton, S. M. Heald, Phys. Rev. B 49, 3709, 1994.